arXiv:1609.09060v1 [cond-mat.dis-nn] 28 Sep 2016

Exact Machine Learning Topological States

Dong-Ling Deng, Xiaopeng Li, and S. Das Sarma
Condensed Matter Theory Center and Joint Quantum Institute, Department of Physics, University of Maryland, College Park, MD 20742-4111, USA

Artificial neural networks play a prominent role in the rapidly growing field of machine learning and are recently introduced to quantum many-body systems to tackle complex problems. Here, we find that even topological states with long-range quantum entanglement can be represented with classical artificial neural networks. This is demonstrated by using two concrete spin systems, the one-dimensional (1D) symmetry-protected topological cluster state and the 2D toric code state with an intrinsic topological order. For both cases we show rigorously that the topological ground states can be represented by short-range neural networks in an *exact* fashion. This neural network representation, in addition to being exact, is surprisingly *efficient* as the required number of hidden neurons is as small as the number of physical spins. Our exact construction of topological-order neuron-representation demonstrates explicitly the exceptional power of neural networks in describing exotic quantum states, and at the same time provides valuable topological data to supervise machine learning topological quantum orders in generic lattice models.

Machine learning, grown out of the quest for artificial intelligence, is one of today's most active fields across disciplines with vast applications ranging from fundamental research in cheminformatics, biology, and cosmology to quantitative social sciences [1, 2]. Within physics, machine learning techniques have been vigorously used in gravitational wave analysis [3, 4], black hole dectection [5], classification of liquid-glass transitions [6], and material design [7]. Very recently, these techniques have been utilized to study strongly correlated systems and quantum phase transitions [8–12]. However, previous studies in this context focus on numerical simulations with generic unknown properties due to lack of exact results. Here, we provide *exact results*, showing that topological states of matter can be represented by artificial neural networks both efficiently and precisely.

In general, to fully describe an arbitrary quantum many-body state requires a huge amount of information due to the exponential scaling of the Hilbert space dimension [13]. Yet, typical physical states may only access a tiny corner of the Hilbert space and in principle could be represented in a much restricted subspace of reduced dimension. For example, the area law entangled quantum states, such as ground states of one-dimensional (1D) local gapped Hamiltonians [14] or the eigenstates of many-body localized systems [15], can be efficiently represented in terms of matrix product states (MPS) [16–18] or tensor-network states in general [19–21]. These compact representations of quantum states grant efficient classical algorithms to solve complex quantum many-body problems, e.g., DMRG (density-matrix renormalization group)[18, 22–24], PEPS [20, 21] (projected entangled pair states), and MERA (multiscale entanglement renormalization ansatz) methods [25, 26]. Recently, an artificial-neural-network representation has been proposed as a completely different route to implement "Hilbert-space reduction" [27], which opens up a new thrust of machine-learning based algorithms to simulate quantum many-body systems. Neural networks have also been successfully exploited in modeling thermodynamic observables [11] and identifying fermionic phases where the traditional quantum Monte Carlo approach fails due to the severe sign problem [12].

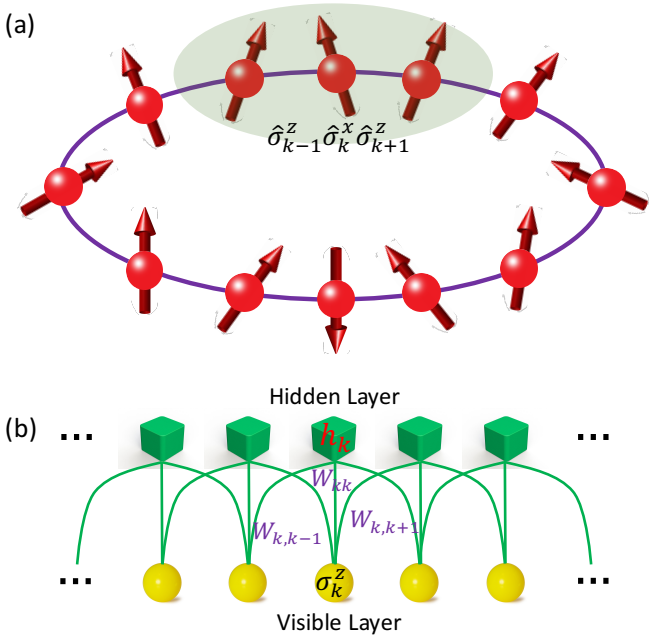

FIG. 1: Representing the 1D symmetry-protected topological cluster state with a neural network. (a) A pictorial illustration of the 1D cluster Hamiltonian (see Eq. (1)) with the periodic boundary condition. The shaded region represents a prototypic three-body interaction (a stabilizer) at an arbitrary site k. (b) A short-range neural network representation of the 1D topological cluster state. The yellow balls (blue cubes) denote the visible (hidden) artificial neurons.

Although the existence of a neural network representation of arbitrary quantum states is assured by mathematical theorems [28–30], how the required classical resources

scale is *unknown*, particularly for exotic nonlocal quantum states with nontrivial entanglement properties such as topological phases [31–35]. Whether the long-range entanglement and the computational power of topological states, via topological quantum computing [36–38], intrinsically prohibit an efficient neural network representation in a classical learning machine is an open question of particular interest to the interdiscipline of quantum condensed matter physics and classical machine learning. In this work, we establish the answer to this question to be *no*, by using two concrete examples, one concerning the 1D symmetry-protected topological (SPT) cluster state [39] and the other being the 2D toric code state with intrinsic topological order [37]. For both models, we provide exact and efficient neural-network representations (see Fig. 1 and Fig. 2) explicitly. Our analytic construction provides valuable data resources to help supervise classical machine learning quantum topological phases in generic non-solvable lattice models as well.

Artificial-neural-network representation.—To begin with, let us first outline the artificial-neural-network representation of quantum states, which has recently been introduced by Carleo and Troyer in solving many-body problems via machine learning ideas [27]. Considering a quantum system with N spins $\Xi = (\sigma_1, \sigma_2, \cdots \sigma_N)$, we use the restricted Boltzmann machine (RBM), which is a stochastic artificial neural network with widespread applications [40–45], to describe the many-body wavefunction $\Phi(\Xi)$. We focus on spin-1/2 quantum systems. The RBM contains two layers [28], one visible layer of N nodes corresponding to the physical spins, and the other a hidden layer of M auxiliary classical spin variables $h_1, \cdots, h_M$ (see Fig. 1(b) for an 1D example). An artificial-neural-network quantum state (ANNQS) has the form [27]: $\Phi_M(\Xi;\Omega) = \sum_{\{h_k\}} e^{\sum_k a_k\sigma_k^z + \sum_{k'} b_{k'}h_{k'} + \sum_{kk'} W_{kk'}h_k\sigma_{k'}^z}$, where $\{h_k\} = \{-1,1\}^M$ denotes the possible configurations of M hidden auxiliary spins and the weights $\Omega = (a_k, b_{k'}, W_{kk'})$ are parameters needed to train to best represent the many-body quantum state. ANNQS should be taken as a variational state and for a given $\Phi_M(\Xi;\Omega)$, the actural quantum many-body state $|\Phi\rangle$ is understood as (up to an irrelevant normalization constant) $|\Phi\rangle = \sum_\Xi \Phi_M(\Xi;\Omega)|\Xi\rangle$, similar to the Laughlin-like representation of the exact resonating-valence-bond ground state of the Haldane-Shastry model [46, 47].

While the representability theorems guarantee the existence of ANNQS to *approximate* arbitrary many-body state [28–30], such existence would not be practically useful if an exponential (in system size) number of neurons are required. Moreover, given a specific quantum system, there is so far no systematic way to write down its wave function in terms of ANNQS other than using the numerically costly reinforcement training method. It is thus desirable to construct *exact* ANNQS for non-trivial quantum many-body systems. In this work, we show how to use ANNQS to represent certain topological states exactly and efficiently (in the sense that both the number of neurons and the number of weight variables are linear in system size). We give two explicit examples, one for the SPT cluster state in 1D and the other for the 2D torric code state with intrinsic topological order.

1D SPT cluster state.—We consider the following Hamiltonian defined on a 1D lattice with periodic boundary condition (Fig. 1a):

$$H_{\text{cluster}} = -\sum_{k=1}^{N} \hat{\sigma}_{k-1}^z \hat{\sigma}_k^x \hat{\sigma}_{k+1}^z, \tag{1}$$

where $\hat{\sigma}^z$ and $\hat{\sigma}^x$ are Pauli matrices and N denotes the system size. Throughout this paper, we use $\hat{\bullet}$ for operators (e.g., $\hat{\sigma}^z$ and $\hat{\sigma}^x$) and σ^z for classical variables ($\sigma^z = \pm 1$). The Hamiltonian H_{cluster} has two Z_2 symmetries corresponding to $\hat{\sigma}^{z,y} \to -\hat{\sigma}^{z,y}$ for either even- or odd-indexed sites, and its ground state is a topological state protected by $Z_2 \times Z_2$ symmetry [39], analogous to the Haldane phase of the spin-1 chain [48–50]. Due to the stabilizer nature of the Hamiltonian, the ground state $|G\rangle$ obeys

$$\hat{\sigma}_{k-1}^z \hat{\sigma}_k^x \hat{\sigma}_{k+1}^z |G\rangle = |G\rangle, \quad \forall k. \tag{2}$$

In the context of quantum information and computation, this state $|G\rangle$ is called a cluster state [51] or more generally a graph state [52]. It has important applications in measurement-based quantum computation [52–54]. We note that a variant of H_{cluster} has also been studied recently in the context of many-body localization, where the symmetry protected topological phase is shown to persist even to highly excited eigenstates due to localization protection [55].

Here we construct an exact artificial neural network representation for the cluster state. Before we provide details of the construction and derivation, we first outline the main steps. A brute-force construction of the ANNQS wave function in principle involves dealing with infinite number of variables and possibilities. To simplify the problem, we assume a further restricted RBM structure as shown in Fig. 1(b). We then use the constraint set by Eq. (2) and build up a series of equations which the variational parameters in the ANNQS must satisfy. As the number of equations is actually more than that of variational parameters, we solve these equations with an optimization method. The existence of a solution in this overdetermined problem (to be presented later) validates our approach.

In the ANNQS representation, we have $|G\rangle = \sum_\Xi \Phi_M(\Xi;\Omega)|\Xi\rangle$. Then Eq. 2 gives,

$$\hat{\sigma}_{k-1}^z \hat{\sigma}_k^x \hat{\sigma}_{k+1}^z \sum_\Xi \Phi_M(\Xi;\Omega)|\Xi\rangle = \sum_\Xi \Phi_M(\Xi;\Omega)|\Xi\rangle. \tag{3}$$

Our aim is to design a network and solve the weight variables Ω to satisfy the above equation for all k. Noting that the operator $\hat{\sigma}_k^x$ will flip spin on site k and $\hat{\sigma}_j^z|\Xi\rangle = \sigma_j^z|\Xi\rangle$, we can reduce Eq. (3) to

$$\Phi_M(\Xi;\Omega)\sigma_{k-1}^z\sigma_{k+1}^z \;=\; \Phi_M(\Xi,\sigma_k^z\to-\sigma_k^z;\Omega). \quad (4)$$

Noting that the RBM contains no intra-layer connections, we can explicitly factor out the hidden variables and rewrite $\Phi_M(\Xi;\Omega)$ in a product form: $\Phi_M(\Xi;\Omega) = \prod_{k=1}^N e^{a_k\sigma_k^z}\prod_{k'=1}^M \Gamma_{k'}(\Xi)$, with $\Gamma_{k'}(\Xi) = 2\cosh[b_{k'} + \sum_k W_{k'k}\sigma_k^z]$. As a consequence, Eq. (4) can be rewritten as

$$\sigma_{k-1}^z\sigma_{k+1}^z\prod_{j=1}^N e^{a_j\sigma_j^z}\prod_{l=1}^M 2\cosh[b_l+\sum_{k'}W_{lk'}\sigma_{k'}^z] = e^{-a_k\sigma_k^z} \times\prod_{j\neq k}^N e^{a_j\sigma_j^z}\prod_{l=1}^M 2\cosh[b_l+\sum_{k'\neq k}W_{lk'}\sigma_{k'}^z - W_{lk}\sigma_k^z], \quad (5)$$

which is the essential equation to determine the actual neural network. An exact representation of $|G\rangle$ requires Eq. (5) to be satisfied for all spin configurations Ξ and all k. This gives us a series of (on the order of $\sim N2^N$) highly nonlinear equations, which is hard to solve directly for general neural networks. With a finite number of neurons, it is unknown whether a solution even exists. We will thus not attempt to solve the problem for a general neural network. Instead, we will work in an alternate direction. We first choose a simple specific network with a small number of neurons (linear in system size) and a few nonzero parameters. If no solution to Eq. (5) can be obtained, we then try enlarging the search space with more neurons and more nonzero parameters, and repeat the procedure until Eq. (5) is satisfied. Fortunately, it turns out that for the two examples given in this paper, exact solutions can indeed be obtained with moderate efforts if we choose the networks deliberately using this simple systematic approach.

Since the cluster state $|G\rangle$ has translational invariance and is short-range entangled (formally it has area law entanglement entropy [14]), a natural guess of the RBM representation for $|G\rangle$ has a further restricted form with the inter-layer neurons locally coupled as shown in Fig. 1(b), where the number of hidden-neurons is equal to the lattice size N. In the corresponding reduced ANNQS wave function, the weight parameters are chosen to be

$$a_k = 0,\; b_k = ib,\; W_{kj} = \begin{cases} i\omega_{k-j}, & \text{if } |k-j|=1 \\ 0 & \text{otherwise} \end{cases}. \quad (6)$$

Here we choose the parameters to be purely imaginary to convert the hyperbolic cosine functions to cosine functions. By plugging Eq. (6) into Eq. (5) and canceling all the equal factors at both sides, we arrive at

$$\sigma_{k-1}^z\sigma_{k+1}^z\Lambda_{k-1}\Lambda_k\Lambda_{k+1} = \Lambda_{k-1}^-\Lambda_k^-\Lambda_{k+1}^-, \quad (7)$$

where $\Lambda_p = \cos[\pi(b+\omega_1\sigma_{p-1}^z+\omega_0\sigma_p^z+\omega_{-1}\sigma_{p+1}^z)]$ $(p = k-1,k,k+1)$ and $\Lambda_p^- = \Lambda_p(\sigma_k^z\to-\sigma_k^z)$. Eq.(7) should be satisfied for any spin configurations of $\Xi_{\rm sub} = (\sigma_{k-2}^z,\sigma_{k-1}^z,\sigma_k^z,\sigma_{k+1}^z,\sigma_{k+2}^z)$, giving rise to a set of 2^5 equations. Directly solving these highly-nonlinear equations is still daunting. But we can recast it as an optimization problem. We define a function $f(b,\omega_1,\omega_0,\omega_{-1}) = \sum_{\Xi_{\rm sub}}(L_{\Xi_{\rm sub}} - R_{\Xi_{\rm sub}})^2$ where $L_{\Xi_{\rm sub}}$ $(R_{\Xi_{\rm sub}})$ denotes the left (right) side of Eq. (7) with configuration $\Xi_{\rm sub}$, and then numerically minimize f over $(b,\omega_1,\omega_0,\omega_{-1})$. A zero minimum of f corresponds to a desired solution to Eq. (7), and we find $(b,\omega_1,\omega_0,\omega_{-1}) = \frac{\pi}{4}(1,2,3,1)$. The corresponding ANNQS representation of $|G\rangle$ is now obtained,

$$\Phi_M(\Xi;\Omega) \;=\; \sum_{\{h_k\}} e^{\frac{i\pi}{4}\sum_k h_k(1+2\sigma_{k-1}^z+3\sigma_k^z+\sigma_{k+1}^z)}. \quad (8)$$

This gives a compact neural network representation of the cluster state whose number of nonzero parameters scales linearly with the system size($\sim 4N$). We stress that our RBM-based representation for the SPT cluster ground state is *exact* as the corresponding ANNQS satisfies Eq. (2) exactly, despite the restriction we have made.

2D Kitaev toric code state.—As our second example, we study the toric code model [37], which was introduced by Kitaev [37] in the context of topological quantum computation [36] and quantum error correction [57]. This model gives the simplest and most well studied spin liquid ground state that has an intrinsic Z_2 topological order [58, 59]. Considering a $L\times L$ square lattice with the periodic boundary condition (a 2D torus $\mathbb{T}^2$) with each edge of the lattice attached a qubit (Fig. 2). We have $N = 2L^2$ qubits in total. For each vertex $\mathcal{V}$ (face $\mathcal{F}$) (see Fig. 2(a)) we define a vertex (face) operator $A_\mathcal{V} = \prod_{k\in\mathcal{V}}\hat{\sigma}_k^x$ $(B_\mathcal{F} = \prod_{k\in\mathcal{F}}\hat{\sigma}_k^z)$, which are also called stabilizers in quantum error correction language. The model Hamiltonian reads:

$$H_{\rm Kitaev} \;=\; -\sum_{\mathcal{V}\in\mathbb{T}^2}A_\mathcal{V} - \sum_{\mathcal{F}\in\mathbb{T}^2}B_\mathcal{F}. \quad (9)$$

This model is exactly solvable since all the four-body operators in $H_{\rm Kitaev}$ commute with each other. It can be interpreted as a particular Ising lattice gauge theory [60] with an abelian Z_2 gauge group [61]. Its ground state is four-fold degenerate, a signature of intrinsic topological order. The low-energy excitations are abelian anyons with nontrivial mutual statistics [37]. Because of its fundamental importance in the studies of quantum computing and topological phases of matter, the toric code has attracted tremendous interest in both theory [56, 61–64] and experiment [65–69]. The ground state of the model satisfies $B_\mathcal{F}|G_{\rm toric}\rangle = |G_{\rm toric}\rangle$ and $A_\mathcal{V}|G_{\rm toric}\rangle = |G_{\rm toric}\rangle$. Here, we show that $|G_{\rm toric}\rangle$ has an *exact* and *efficient* neural-network representation. We present the result and the verification here and provide

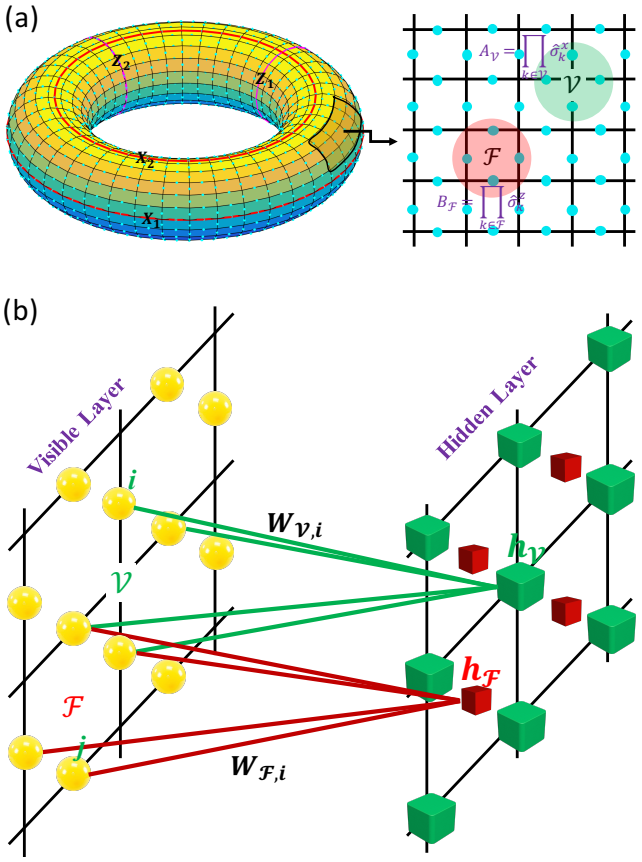

FIG. 2: The 2D Kitaev toric code Hamiltonian and a neural-network representation of the corresponding ground state with intrinsic topological order. (a) An illustration of H_{Kitaev} (see Eq. (9)). The shaded green (red) region depicts a prototypic vertex (face) operator at vertex $\mathcal{V}$ (face $\mathcal{F}$). The Hamiltonian is defined as a summation of these four-body operators with an extra minus sign in front. The four non-contractible loops (labeled by X_1, X_2, Z_1 and Z_2, respectively) correspond to four nontrivial string operators that define the commutation relations of the two logic qubits living in the topologically protected ground subspace [37, 56]. (b) A neural-network representation of one of the ground state of H_{Kitaev}. The yellow balls stand for the visible artificial neurons corresponding to the physical spins. The green (red) cubes denotes the hidden neurons corresponding to the vertices (faces).

the more involved construction details in the Supplemental Material [70]. As illustrated in Fig. 2, the artificial neural network representation of the toric code ground state, $|G_{\text{toric}}\rangle = \sum_\Xi \Phi_M(\Xi)|\Xi\rangle$, is given by

$$\Phi_M(\Xi) = \sum_{\{h_\mathcal{V}, h_\mathcal{F}\}} e^{\frac{i\pi}{2}\sum_\mathcal{V} h_\mathcal{V} \sum_{j\in\mathcal{V}} \sigma_j^z + \frac{i\pi}{4}\sum_\mathcal{F} h_\mathcal{F} \sum_{k\in\mathcal{F}} \sigma_k^z}.$$

To verify the the exact nature of our solution, as done in the 1D example, we can factor out the hidden neurons, $\Phi_M(\Xi;\Omega) = \prod_\mathcal{V} \cos[\frac{\pi}{2}(\sum_{j\in\mathcal{V}} \sigma_j^z)] \prod_\mathcal{F} \cos[\frac{\pi}{4}(\sum_{j\in\mathcal{F}} \sigma_j^z)]$. Noting that $\cos[\frac{\pi}{4}\sum_{j\in\mathcal{F}} \sigma_j^z] \prod_{k\in\mathcal{F}} \sigma_k^z = \cos[\frac{\pi}{4}\sum_{j\in\mathcal{F}} \sigma_j^z]$, the equation $B_\mathcal{F}|G_{\text{toric}}\rangle = |G_{\text{toric}}\rangle$ can be easily verified. In order to verify $A_\mathcal{V}|G_{\text{toric}}\rangle = |G_{\text{toric}}\rangle$, we need to show $\Phi_M(\Xi) = \Phi_M(\Xi, \sigma_j^z \to -\sigma_j^z, \forall j \in \mathcal{V})$. This actually follows from two observations about the consequence of flipping spins belonging to a vertex $\mathcal{V}$, which are the sign-change of all four cosine factors for the neighboring vertices $\mathcal{V}$s and the sign-preservation of the product of the four cosine factors for the neighboring faces $\mathcal{F}$s.

Conclusion and discussion.—In summary, we have demonstrated by using two concrete examples that quantum topological states (both symmetry protected and intrinsic) can be efficiently represented by classical artificial neural networks. We have constructed exact representations for an SPT state (the 1D cluster state) and an intrinsic topologically ordered state (the 2D toric code), by using a *restricted* RBM neural networks method. For both cases, the number of neurons in the hidden layer of the RBM is equal to the number of physical spins, and the number of nonzero weight variables scales linearly with system size. We expect that our construction carries over to the 3D torric code model [71] and the 3D time-reversal SPT phase of bosons with intrinsic surface topological order [72]. In the future, it would be particularly interesting to find exact and efficient examples of neural-network representation of quantum many-body states with volume-law entanglement, which cannot be described in terms of matrix product states or tensor-network states with a computationally tractable bond dimension.

Our results manifest the remarkable power of neural networks in describing exotic quantum states and thus would have far-reaching implications in the applications of machine learning techniques in condensed matter physics. The fact that we obtain an efficient solution is perhaps not as surprising as the fact that our highly-restricted neural network solution turns out to be exact. Our exact results should provide valuable data resources to supervise classical machine learning of topological phases of quantum matter in other models with no known exact solutions, which may be particularly useful considering the potential NP complexity of the numerical training of the RBM for exotic quantum systems. In turn, this may also help the study of machine learning itself, especially in the efforts toward understanding why machine learning techniques are surprisingly powerful [44, 73], from a physical perspective.

Acknowledgment.— DLD thanks Y. L. Wu for helpful discussions. This work is supported by JQI- NSF-PFC and LPS-MPO-CMTC.

[1] M. Jordan and T. Mitchell, Science **349**, 255 (2015).
[2] Y. LeCun, Y. Bengio, and G. Hinton, Nature **521**, 436 (2015).
[3] R. Biswas, L. Blackburn, J. Cao, R. Essick, K. A. Hodge, E. Katsavounidis, K. Kim, Y.-M. Kim, E.-O. Le Bigot, C.-H. Lee, J. J. Oh, S. H. Oh, E. J. Son, Y. Tao, R. Vaulin, and X. Wang, Phys. Rev. D **88**, 062003

(2013).
[4] B. P. Abbott *et al.* (LIGO Scientific Collaboration and Virgo Collaboration), Phys. Rev. Lett. **116**, 061102 (2016).
[5] M. Pasquato, arXiv:1606.08548 (2016).
[6] S. S. Schoenholz, E. D. Cubuk, D. M. Sussman, E. Kaxiras, and A. J. Liu, Nat. Phys. (2016), 10.1038/nphys3644.
[7] S. V. Kalinin, B. G. Sumpter, and R. K. Archibald, Nat. Mater. **14**, 973 (2015).
[8] L.-F. Arsenault, O. A. von Lilienfeld, and A. J. Millis, arXiv:1506.08858 (2015).
[9] J. Carrasquilla and R. G. Melko, arXiv:1605.01735 (2016).
[10] L. Wang, arXiv:1606.00318 (2016).
[11] G. Torlai and R. G. Melko, arXiv:1606.02718 (2016).
[12] P. Broecker, J. Carrasquilla, R. G. Melko, and S. Trebst, arXiv:1608.07848 (2016).
[13] S. Gharibian, Y. Huang, Z. Landau, and S. W. Shin, Found. Trends Theor. Comput. Sci. **10**, 159 (2015).
[14] M. B. Hastings, J. Stat. Mech. , P08024 (2007).
[15] M. Friesdorf, A. H. Werner, W. Brown, V. B. Scholz, and J. Eisert, Phys. Rev. Lett. **114**, 170505 (2015).
[16] M. Fannes, B. Nachtergaele, and R. F. Werner, Comm. Math. Phys. **144**, 443 (1992).
[17] D. Perez-Garcia, F. Verstraete, M. Wolf, and J. Cirac, Quantum Inf. Comput. **7**, 401 (2007).
[18] U. Schollwöck, Ann. of Phys. **326**, 96 (2011).
[19] Z.-C. Gu and X.-G. Wen, Phys. Rev. B **80**, 155131 (2009).
[20] R. Orús, Annals of Physics **349**, 117 (2014).
[21] F. Verstraete, V. Murg, and J. I. Cirac, Advances in Physics **57**, 143 (2008).
[22] S. R. White, Phys. Rev. Lett. **69**, 2863 (1992).
[23] U. Schollwöck, Rev. Mod. Phys. **77**, 259 (2005).
[24] G. Vidal, Phys. Rev. Lett. **91**, 147902 (2003).
[25] G. Vidal, Phys. Rev. Lett. **99**, 220405 (2007).
[26] G. Vidal, Phys. Rev. Lett. **101**, 110501 (2008).
[27] G. Carleo and M. Troyer, arXiv:1606.02318 (2016).
[28] N. Le Roux and Y. Bengio, Neural Comput. **20**, 1631 (2008).
[29] K. Hornik, Neural networks **4**, 251 (1991).
[30] A. N. Kolmogorov, Amer. Math. Soc. Transl **28**, 55 (1963).
[31] X.-G. Wen, *Quantum field theory of many-body systems: from the origin of sound to an origin of light and electrons* (Oxford University Press, 2004).
[32] X. Chen, Z.-C. Gu, Z.-X. Liu, and X.-G. Wen, Science **338**, 1604 (2012).
[33] C.-K. Chiu, J. C. Y. Teo, A. P. Schnyder, and S. Ryu, Rev. Mod. Phys. **88**, 035005 (2016).
[34] X.-L. Qi and S.-C. Zhang, Rev. Mod. Phys. **83**, 1057 (2011).
[35] M. Z. Hasan and C. L. Kane, Rev. Mod. Phys. **82**, 3045 (2010).
[36] C. Nayak, S. H. Simon, A. Stern, M. Freedman, and S. Das Sarma, Rev. Mod. Phys. **80**, 1083 (2008).
[37] A. Y. Kitaev, Ann. Phys. **303**, 2 (2003).
[38] A. Kitaev, Ann. Phys. **321**, 2 (2006).
[39] W. Son, L. Amico, and V. Vedral, Quantum Information Processing **11**, 1961 (2012).
[40] G. E. Hinton and R. R. Salakhutdinov, Science **313**, 504 (2006).
[41] R. Salakhutdinov, A. Mnih, and G. Hinton, in *Proceedings of the 24th international conference on Machine learning* (ACM, 2007) pp. 791–798.
[42] H. Larochelle and Y. Bengio, in *Proceedings of the 25th international conference on Machine learning* (ACM, 2008) pp. 536–543.
[43] M. H. Amin, E. Andriyash, J. Rolfe, B. Kulchytskyy, and R. Melko, arXiv:1601.02036 (2016).
[44] P. Mehta and D. J. Schwab, arXiv:1410.3831 (2014).
[45] S. H. Adachi and M. P. Henderson, arXiv:1510.06356 (2015).
[46] F. D. M. Haldane, Phys. Rev. Lett. **60**, 635 (1988).
[47] B. S. Shastry, Phys. Rev. Lett. **60**, 639 (1988).
[48] F. D. M. Haldane, Phys. Rev. Lett. **50**, 1153 (1983).
[49] I. Affleck, T. Kennedy, E. H. Lieb, and H. Tasaki, Phys. Rev. Lett. **59**, 799 (1987).
[50] I. Affleck, T. Kennedy, E. H. Lieb, and H. Tasaki, Comm. Math. Phys. **115**, 477 (1988).
[51] H. J. Briegel and R. Raussendorf, Phys. Rev. Lett. **86**, 910 (2001).
[52] M. Hein, J. Eisert, and H. J. Briegel, Phys. Rev. A **69**, 062311 (2004).
[53] R. Raussendorf, D. E. Browne, and H. J. Briegel, Phys. Rev. A **68**, 022312 (2003).
[54] M. A. Nielsen, Rep. Math. Phys. **57**, 147 (2006).
[55] Y. Bahri, R. Vosk, E. Altman, and A. Vishwanath, Nat. Comm. **6** (2015), 10.1038/ncomms8341.
[56] M.-G. Hu, D.-L. Deng, and J.-L. Chen, Phys. Rev. A **79**, 010301 (2009).
[57] D. A. Lidar and T. A. Brun, *Quantum error correction* (Cambridge University Press, 2013).
[58] N. Read and S. Sachdev, Phys. Rev. Lett. **66**, 1773 (1991).
[59] X. G. Wen, Phys. Rev. B **44**, 2664 (1991).
[60] J. B. Kogut, Rev. Mod. Phys. **51**, 659 (1979).
[61] A. Kitaev and C. Laumann, Exact Methods in Low-dimensional Statistical Physics and Quantum Computing: Lecture Notes of the Les Houches Summer School: Volume 89, July 2008 **89**, 101 (2010).
[62] L.-M. Duan, E. Demler, and M. D. Lukin, Phys. Rev. Lett. **91**, 090402 (2003).
[63] M. Aguado, G. K. Brennen, F. Verstraete, and J. I. Cirac, Phys. Rev. Lett. **101**, 260501 (2008).
[64] A. Hamma, R. Ionicioiu, and P. Zanardi, Physics Letters A **337**, 22 (2005).
[65] J.-F. Du, J. Zhu, M.-G. Hu, and J.-L. Chen, arXiv:0712.2694 (2007).
[66] S. Gladchenko, D. Olaya, E. Dupont-Ferrier, B. Doucot, L. B. Ioffe, and M. E. Gershenson, Nat. Phys. **5**, 48 (2009).
[67] C.-Y. Lu, W.-B. Gao, O. Gühne, X.-Q. Zhou, Z.-B. Chen, and J.-W. Pan, Phys. Rev. Lett. **102**, 030502 (2009).
[68] J. Pachos, W. Wieczorek, C. Schmid, N. Kiesel, R. Pohlner, and H. Weinfurter, New J. Phys. **11**, 083010 (2009).
[69] Y. P. Zhong, D. Xu, P. Wang, C. Song, Q. J. Guo, W. X. Liu, K. Xu, B. X. Xia, C.-Y. Lu, S. Han, J.-W. Pan, and H. Wang, Phys. Rev. Lett. **117**, 110501 (2016).
[70] See Supplemental Material at [URL will be inserted by publisher] for:.
[71] A. Hamma, P. Zanardi, and X.-G. Wen, Phys. Rev. B **72**, 035307 (2005).
[72] F. J. Burnell, X. Chen, L. Fidkowski, and A. Vishwanath, Phys. Rev. B **90**, 245122 (2014).
[73] H. W. Lin and M. Tegmark, arXiv:1608.08225 (2016).

Supplemental Materials: Exact Machine Learning Topological States

In this Supplementary Materials, we give the details about how we construct the neural network representation of the 2D toric code states with intrinsic topological order.

Noting that all these four-body operators in H_{Kitaev} commute with each other, thus the eigenstates of the Hamiltonian are also the eigenstates of these operators. The ground state satisfies the following equations:

$$B_{\mathcal{F}}|G_{\text{toric}}\rangle = \prod_{j\in\mathcal{F}}\hat{\sigma}_j^z|G_{\text{toric}}\rangle = |G_{\text{toric}}\rangle, \quad \forall\mathcal{F}, \tag{S1}$$

$$A_{\mathcal{V}}|G_{\text{toric}}\rangle = \prod_{j\in\mathcal{V}}\hat{\sigma}_j^x|G_{\text{toric}}\rangle = |G_{\text{toric}}\rangle, \quad \forall\mathcal{V}. \tag{S2}$$

We propose the following neural network state to represent $|G_{\text{toric}}\rangle$:

$$\Phi_M(\Xi;\Omega) = \sum_{\{h_{\mathcal{V}},h_{\mathcal{F}}\}} e^{\sum_k a_k\sigma_k^z+\sum_{\mathcal{V}} b_{\mathcal{V}}h_{\mathcal{V}}+\sum_{\mathcal{F}} b_{\mathcal{F}}h_{\mathcal{F}}+\sum_{\mathcal{V}k} W_{\mathcal{V}k}h_{\mathcal{V}}\sigma_k^z+\sum_{\mathcal{F}k} W_{\mathcal{F}k}h_{\mathcal{F}}\sigma_k^z}, \tag{S3}$$

where $h_{\mathcal{V}}=\{-1,1\}$ ($h_{\mathcal{F}}=\{-1,1\}$) are the set of hidden neurons corresponding to the vertices (faces); the weights $\Omega=(a_k,b_{\mathcal{V}},b_{\mathcal{F}},W_{\mathcal{V}k},W_{\mathcal{F}k})$ are parameters we need to train. The visible neurons corresponding to the physical spins live on edges of the square lattice. Throughout this Supplemental Materials, the lower-case letters (k or j) are used to label individual physical spins (or visible neurons in the restricted Boltzmann machine (RBM) language). For convenience, we also introduce a combined index like $(\mathcal{F},\mu)$, with $\mathcal{F}$ labeling the faces, and μ the spins within each face. As there is no intra-layer connection in the network, we can rewrite the RBM $\Phi_M(\Xi;\Omega)$ in a product form:

$$\Phi_M(\Xi;\Omega) = \prod_{k=1}^{N} e^{a_k\sigma_k^z}\prod_{\mathcal{V}}\Gamma_{\mathcal{V}}(\Xi)\prod_{\mathcal{F}}\Gamma_{\mathcal{F}}(\Xi), \tag{S4}$$

with

$$\Gamma_{\mathcal{V}}(\Xi) = 2\cosh[b_{\mathcal{V}}+\sum_k W_{\mathcal{V}k}\sigma_k^z],$$
$$\Gamma_{\mathcal{F}}(\Xi) = 2\cosh[b_{\mathcal{F}}+\sum_k W_{\mathcal{F}k}\sigma_k^z].$$

To simplify the problem, we introduce a further restriction that the hidden vertex (face) neurons only connect to the visible neurons belonging to the corresponding vertex (face) (with a corresponding rule shown in Fig.2(b) in the main text):

$$W_{\mathcal{V}k} = 0, \quad \text{if } k\notin\mathcal{V}, \tag{S5}$$

$$W_{\mathcal{F}k} = 0, \quad \text{if } k\notin\mathcal{F}. \tag{S6}$$

We need to find out the weight parameters Ω so to make Eq. (S3) represent the ground state of H_{Kitaev}. Since the face operators do not involve spin flip, it is easier to solve Eq. (S1), and then we get $b_{\mathcal{F}}$ and $W_{\mathcal{F}k}$. To this end, we plug Eq. (S4) into Eq. (S1) and obtain

$$\prod_{j\in\mathcal{F}}\sigma_j^z\prod_{k=1}^{N}e^{a_k\sigma_k^z}\prod_{\mathcal{V}}\Gamma_{\mathcal{V}}(\Xi)\prod_{\mathcal{F}'}\Gamma_{\mathcal{F}'}(\Xi) = \prod_{k=1}^{N}e^{a_k\sigma_k^z}\prod_{\mathcal{V}}\Gamma_{\mathcal{V}}(\Xi)\prod_{\mathcal{F}'}\Gamma_{\mathcal{F}'}(\Xi), \quad \forall\mathcal{F}. \tag{S7}$$

Canceling all (except $\Gamma_{\mathcal{F}}(\Xi)$) equal factors on both sides of Eq. (S7), we have

$$\prod_{j\in\mathcal{F}}\sigma_j^z\ \cosh[b_{\mathcal{F}}+\textstyle\sum_{\mu=1}^4 W_{\mathcal{F};(\mathcal{F},\mu)}\sigma_{(\mathcal{F},\mu)}^z] = \cosh[b_{\mathcal{F}}+\sum_{\mu=1}^{4}W_{\mathcal{F};(\mathcal{F},\mu)}\sigma_{(\mathcal{F},\mu)}^z], \quad \forall\mathcal{F}, \tag{S8}$$

where we have used $(\mathcal{F},\mu)$ ($\mu=1,2,3,4$) to denote the four visible neurons belong to $\mathcal{F}$. Noting that $\sum_{\mu=1}^4\sigma_{(\mathcal{F},\mu)}^z = 0,\pm2,\pm4$, it is straightforward to find a solution to Eq. (S8):

$$b_{\mathcal{F}} = 0,\ W_{\mathcal{F};(\mathcal{F},\mu)} = \frac{i\pi}{4}, \quad \forall\mu,\mathcal{F}.$$

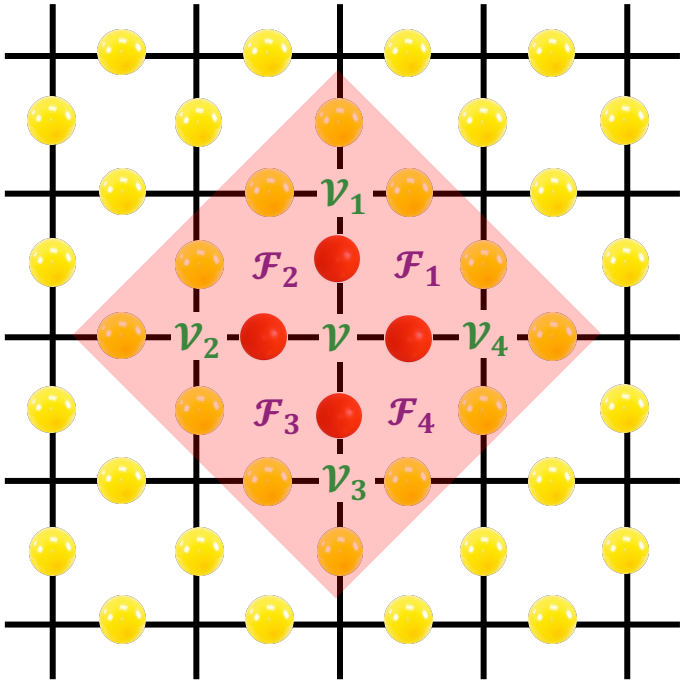

FIG. S1: Affected region for acting the vertex operator $A_\mathcal{V}$. $A_\mathcal{V}$ flips four spins belonging to $\mathcal{V}$ (denoted by the red balls). The shaded region stands for the region that are affected by the spin flip.

We now turn to the more involved case of solving Eq. (S2) to obtain a_k, $b_\mathcal{V}$, and $W_{\mathcal{V}k'}$. Plugging (S4) into Eq. (S2) and fix $a_k = 0$, $\forall k$, we obtain

$$\sum_\Xi \prod_{\mathcal{V}'} \Gamma_{\mathcal{V}'}(\Xi) \prod_\mathcal{F} \Gamma_\mathcal{F}(\Xi) \ \ |\Xi; \sigma_j^z \to -\sigma_j^z, \forall j \in \mathcal{V}\rangle \ = \sum_\Xi \prod_{\mathcal{V}'} \Gamma_{\mathcal{V}'}(\Xi) \prod_\mathcal{F} \Gamma_\mathcal{F}(\Xi) |\Xi\rangle, \ \forall \mathcal{V}.$$

Thus we have

$$\prod_{\mathcal{V}'} \Gamma_{\mathcal{V}'}(\Xi) \prod_\mathcal{F} \Gamma_\mathcal{F}(\Xi) \ = \ \prod_{\mathcal{V}'} \Gamma_{\mathcal{V}'}(\Xi; \sigma_j^z \to -\sigma_j^z, \forall j \in \mathcal{V}) \prod_\mathcal{F} \Gamma_\mathcal{F}(\Xi; \sigma_j^z \to -\sigma_j^z, \forall j \in \mathcal{V}), \ \forall \mathcal{V}. \tag{S9}$$

Let us consider spin flips caused by a given vertex $\mathcal{V}$. This corresponding vertex operator $A_\mathcal{V}$ only flips four spins that belong to $\mathcal{V}$. As shown in Fig. S1, we denote the four vertices (faces) nearest to $\mathcal{V}$ as $\mathcal{V}_1$, $\mathcal{V}_2$, $\mathcal{V}_3$, and $\mathcal{V}_4$ ($\mathcal{F}_1$, $\mathcal{F}_2$, $\mathcal{F}_3$, and $\mathcal{F}_4$). Then by using Eq. (S5), we have

$$\begin{aligned} \Gamma_{\mathcal{V}'}(\Xi) \ &= \ \Gamma_{\mathcal{V}'}(\Xi; \sigma_j^z \to -\sigma_j^z, \forall j \in \mathcal{V}), \text{ for } \mathcal{V}' \neq \mathcal{V}_1, \mathcal{V}_2, \mathcal{V}_3, \text{ or } \mathcal{V}_4, \\ \Gamma_\mathcal{F}(\Xi) \ &= \ \Gamma_\mathcal{F}(\Xi; \sigma_j^z \to -\sigma_j^z, \forall j \in \mathcal{V}), \text{ for } \mathcal{F} \neq \mathcal{F}_1, \mathcal{F}_2, \mathcal{F}_3, \text{ or } \mathcal{F}_4. \end{aligned}$$

Canceling out these equal factors, Eq. (S9) reduces to

$$\Gamma_\mathcal{V}(\Xi) \prod_{\mu=1}^4 \Gamma_{\mathcal{V}_\mu}(\Xi) \Gamma_{\mathcal{F}_\mu}(\Xi) \ = \ \Gamma_\mathcal{V}(\Xi; \sigma_j^z \to -\sigma_j^z, \forall j \in \mathcal{V}) \prod_{\mu=1}^4 \Gamma_{\mathcal{V}_\mu}(\Xi; \sigma_j^z \to -\sigma_j^z, \forall j \in \mathcal{V}) \Gamma_{\mathcal{F}_\mu}(\Xi; \sigma_j^z \to -\sigma_j^z, \forall j \in \mathcal{V}). \tag{S10}$$

Let Ξ'_{sub} denote the spins of the corresponding visible neurons belong to $\mathcal{V}_1$, $\mathcal{V}_2$, $\mathcal{V}_3$, $\mathcal{V}_4$, $\mathcal{F}_1$, $\mathcal{F}_2$, $\mathcal{F}_3$, or $\mathcal{F}_4$ (neurons in the shaded region in Fig. S1). Eq. (S10) should be satisfied for any configurations of Ξ'_{sub}, giving a series of $2^{16} = 65536$ equations. Directly solving these equations is daunting. As discussed in the 1D case in the main text, we can recast Eq. (S10) to an optimization problem and find a solution numerically

$$b_\mathcal{V} \ = \ 0, \ W_{\mathcal{V};(\mathcal{V},\mu)} = \frac{i\pi}{2}, \quad \forall \mu, \mathcal{V}.$$

This gives the exact ANNQS representation of the 2D toric code state in the main text.